Invited Article: Bragg stacks with tailored disorder create brilliant whiteness

D. T. Meiers, M.-C. Heep, and G. von Freymann

Citation: APL Photonics **3**, 100802 (2018); doi: 10.1063/1.5048194
View online: https://doi.org/10.1063/1.5048194
View Table of Contents: http://aip.scitation.org/toc/app/3/10
Published by the American Institute of Physics

Invited Article: Bragg stacks with tailored disorder create brilliant whiteness

D. T. Meiers,[1,a,b] M.-C. Heep,[1,a] and G. von Freymann[1,2]
[1]*Physics Department and Research Center OPTIMAS, Technische Universität Kaiserslautern, 67663 Kaiserslautern, Germany*
[2]*Fraunhofer Institute for Industrial Mathematics ITWM, 67663 Kaiserslautern, Germany*

(Received 11 July 2018; accepted 13 August 2018; published online 29 August 2018)

The scales of white beetles strongly scatter light within a thin disordered network of chitin filaments. There is no comparable artificial material achieving such a high scattering strength within a thin layer of low refractive index material. Several analyses investigated the scattering but could not explain the underlying concept. Here a model system is described, which has the same optical properties as the white beetles' scales in the visible wavelength range. With some modification, it also explains the behavior of the structures in the near infrared range. The comparison of the original structure and the model system is done by finite-difference time-domain calculations. The calculations show excellent agreement with the beetles' scales with respect to the reflectance, the time-of-flight, and the intensity distribution in the far-field.
https://doi.org/10.1063/1.5048194

I. INTRODUCTION

The brilliant whiteness of *Lepidiota stigma* and beetles of genus *Cyphochilus* has recently been intensively studied as the underlying multiple scattering structures belong to the strongest known scatterers made from biological materials.[1–5] Although being one magnitude thinner than artificial white materials with a comparable refractive index, e.g., common white paper, the roughly 7 μm thin beetle scales exhibit a similar whiteness.[1,2] In one of the first papers on this topic, Vukusic *et al.* argued that only a narrow border should separate ordered structures like those of the blue *Morpho* butterflies producing strong coloration from highly scattering white structures, as the materials used and typical dimensions are very similar for the different observed structures.[2] Recent work studied the time-resolved transport properties of single scales, finding highly anisotropic transport properties.[3,4] They established that multiple scattering is unequivocally at the heart of the brilliant whiteness. All of these studies relied on structural information gained from destructive cross sections, e.g., focused-ion beam slicing or histology taken from single beetle scales, which tend to deform the scales.[6,7] Wilts *et al.* recently published deformation free cryo-ptychographic X-ray data obtained at a single beetle scale. This allows for the first time for full modeling of the structure using finite-difference time-domain (FDTD) techniques.[1] They proved that the structure in the beetle scales is evolutionarily optimized for highest scattering with regard to minimized material use and available refractive index contrast. Although most of the structural details are revealed, and scattering structures inspired by the beetle scales have been already fabricated;[8–10] an underlying model structure explaining all observed optical characteristics is still elusive to date. We present such a model based on a composition of small Bragg reflectors with tailored disorder which is able to explain so far all the observed optical properties while being simple enough to allow for technological optimization and scaling.

---

[a]D. T. Meiers and M.-C. Heep contributed equally to this work.
[b]Electronic mail: dmeiers@rhrk.uni-kl.de

II. RESULTS AND DISCUSSION

All previous studies on this subject observed the layered structure of the scales.[1–5] As concluded by Cortese *et al.*, layering is the key to achieve high scatterer density while avoiding the detrimental effect of optical crowding.[4] In nature, layered structures are well known for providing brilliant angle-independent coloration, e.g., the brilliant blue appearance of the *Morpho* butterflies.[11–13] Figure 1 exhibits how to achieve such a coloration with a layered structure. A strictly periodic stack [Fig. 1(a)] composed of alternating chitin and air layers with suitable layer thicknesses [$d_{\text{chitin (morpho)}} = 80$ nm and $d_{\text{air (morpho)}} = 102$ nm with $n_{\text{chitin}} = 1.55$ according to Leertouwer *et al.*[14]] shows a high reflectance for blue light but only for a small range of observation angles. According to the well-known building principle of the *Morpho* butterfly scales' structure, this stack is first divided into stacks with sub-wavelength footprint and then adjacent stacks are shifted by half a period.[15,16] Adding a Gaussian distributed offset to every pair consisting of two adjacent stacks leads to the structure sketched in Fig. 1(b). The calculation of the coloration of the far-field (see Sec. IV) shown in Fig. 1(c) clearly reveals the blue appearance over a broad range of observation angles. Since the coloration of the far-field only allows to assess the scattering qualitatively, we calculate the total integrated scattering (TIS) to evaluate the scattering also quantitatively. The TIS is defined as $\text{TIS} = (R_t - R_s)/R_t$, where R_t is the total reflectance and R_s is the specular reflectance.[17] We receive $\text{TIS} = 70.7\% \pm 0.9\%$ for the structure shown in Fig. 1(b) in distinct contrast to $\text{TIS} = 12.9\% \pm 2.2\%$ for the structure shown in Fig. 1(a). This verifies that the introduced disorder improves the scattering and is responsible for the almost angle-independent coloration.

Besides brilliantly colored animals, there are also several other animals whose appearance arises from layered structures. These structures are stacks with varying layer thickness and/or varying layer distance and a large footprint compared to the wavelength exhibiting a broadband reflectance and low scattering, leading to a metallic gold or silver appearance.[18–22] Since a white appearance requires broadband reflectance and strong scattering, we assume that the beetle scales' structure is composed of stacks which combine varying layer thickness with a small footprint and structural disorder.

We analyze the high-resolution tomographic cross section of a white beetle scale reported by Wilts *et al.*[1] The replacement of the chitin layers with a simple block of fitting thickness reveals the varying layer thickness and the small footprint, as shown in Fig. 2(a), exemplary for one position. By adapting this pattern to other parts of the cross section, it can be seen that the structure is composed of many of these small disordered stacks.

Based on this analysis, we develop a model to mimic the beetle scales' structure. The evolution of this model is shown in Figs. 2(b)–2(e). We start with a Bragg stack [Fig. 2(b)] where the thickness of the chitin layer is chosen equal to the mean value of the strut diameter distribution of the scale network provided by Wilts *et al.* and the thickness of the air layer is chosen suitable [$d_{\text{chitin (beetle)}} = 230$ nm and $d_{\text{air (beetle)}} = 357$ nm].[1] First, we vary the layer thickness according to the strut diameter

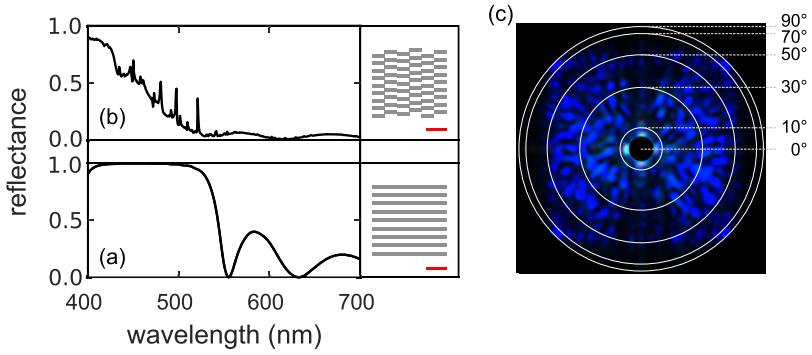

FIG. 1. (a) 2D sketch of a strictly periodic stack of alternating layers (right) and associated calculated reflectance (left). (b) 2D sketch of the *Morpho*-like structure (right) and resulting calculated reflectance for perpendicular incident light (left). (c) Calculated coloration of the far-field for the *Morpho*-like structure sketched in (b) (the specular amount is cut out, black circle). The white circles indicate different azimuthal angles. [(a) and (b)] Scale bars: 500 nm.

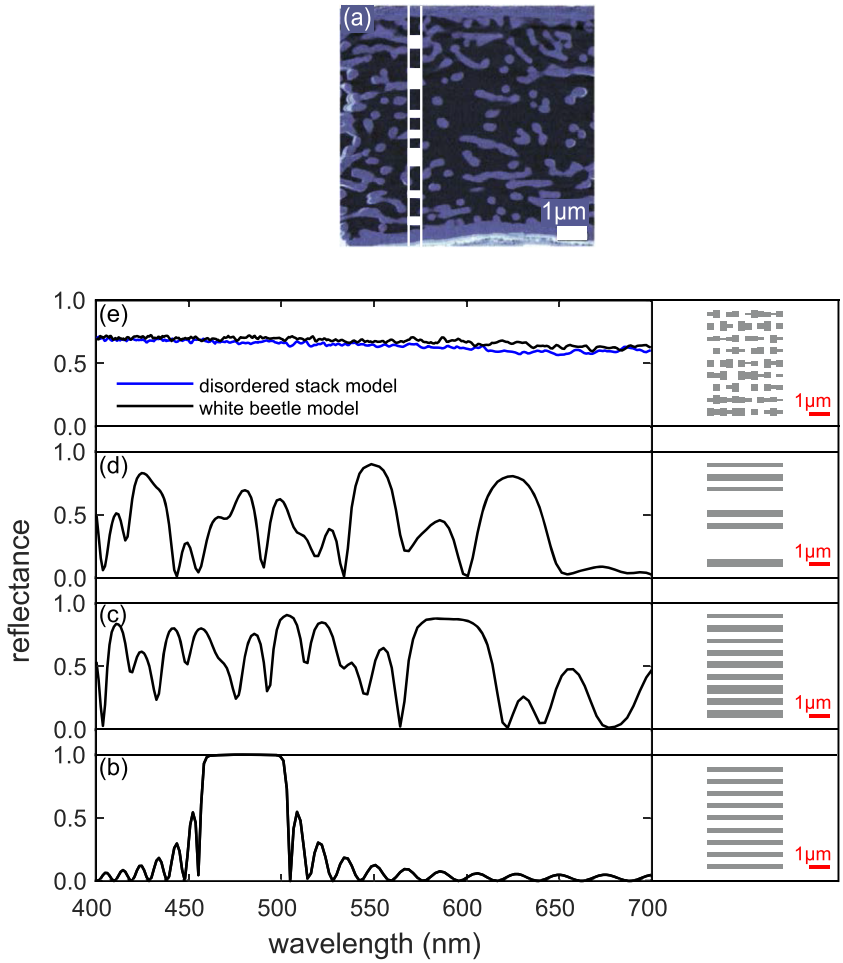

FIG. 2. (a) High resolution tomography slice provided by Wilts *et al.*[1] with a layered like structure highlighted in white. (b)–(e) show each time a 2D sketch (right) and the associated calculated reflectance (left) for (b) a periodic Bragg stack; (c) the same as (b) but with a distributed layer thickness; (d) the same as (c) but with randomly left out layers; (e) composition of different stacks with distributed layer thicknesses and randomly left out layers. (e) Additionally, calculated reflectance for the white beetle model provided by Wilts *et al.* (black line).

distribution (for parameters, see Sec. IV), while the center-to-center distance of the chitin layers is fixed [Fig. 2(c)]. Then, we leave out one-third of the layers randomly [Fig. 2(d)] since the analysis of the cross section [Fig. 2(a)] reveals particular bigger gaps between consecutive blocks because of missing layers. This structural disorder improves the scattering like the shifted layers in the case of the *Morpho* butterflies. Eventually, we compose many of these stacks to achieve the model [Fig. 2(e)]. Thereby, all small stacks are different because of the Gaussian distributed layer thickness and the randomly removed layers. The footprint of the fundamental building blocks is chosen to be small enough to provide strong scattering and big enough to avoid optical crowding. Our model has the same thickness as the white beetle model provided by Wilts *et al.* (7 μm). To compare the optical behavior of both models, we perform FDTD calculations.

Figure 2(e) shows the comparison of the wavelength-dependent reflectance for our model (blue line) and the beetle scales' structure (black line). It can be seen that our model exhibits almost the same behavior like the scales' structure in respect of the reflectance over the entire visible wavelength range.

Since the underlying Bragg stack has a first order stop band at λ = 1426 nm, we expect high reflectance in the near infrared wavelength range for the white beetle, too. Figure 3(a) shows the reflectance in the infrared range for our model and the white beetle model in blue and black,

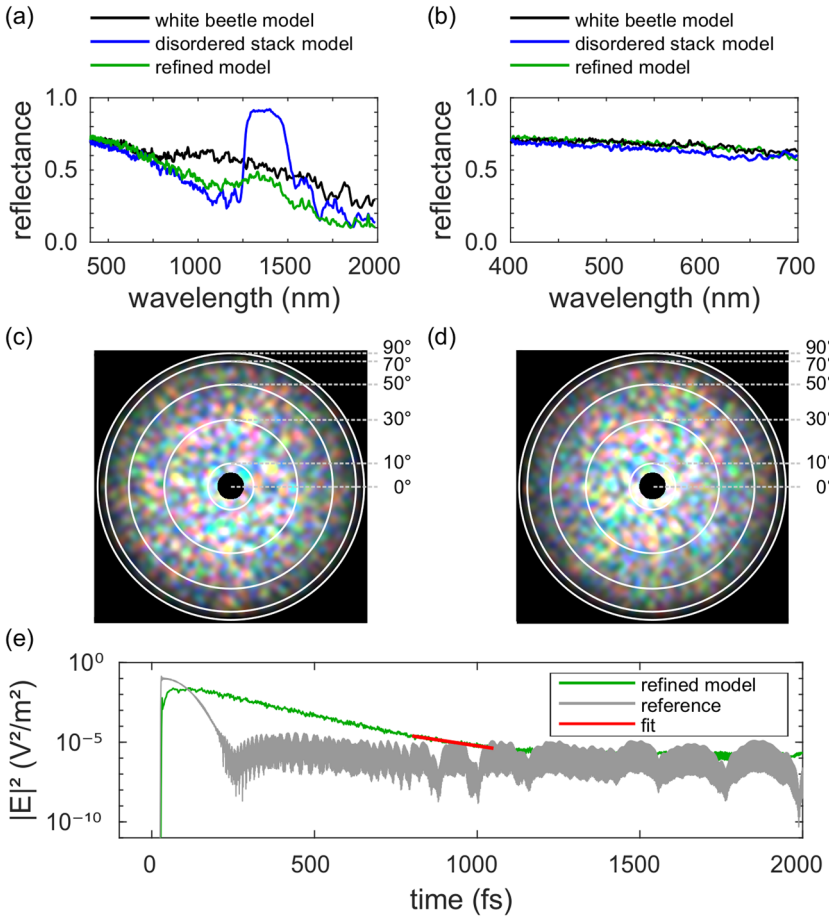

FIG. 3. (a) Comparison of the reflectance for the first model (blue line), the refined model (green line), and the white beetle model (black line) in the visible and near infrared wavelength ranges. (b) Comparison of the reflectance of the first model (blue line), the refined model (green line), and the white beetle model (black line) in the visible wavelength range. (c) Calculated coloring of the far-field for the refined model and (d) for the white beetle model (the specular amount is cut out each time, black circle). The white circles indicate different azimuthal angles. (e) Simulation of the time-of-flight of a light pulse transmitted through the refined model (green line) and through vacuum (gray line). The exponential fit (red line) yields a lifetime of roughly $\tau = 140$ fs.

respectively. The model system reveals the predicted maximum in reflectance around $\lambda = 1400$ nm. By contrast, the white beetle model does not show this characteristic maximum but a broader feature. To explain the optical properties in the near infrared range, we have to modify the model system. We introduce additional disorder to our model using normally distributed center-to-center distances instead of constant ones. In contrast to our first model, the refined model [Fig. 3(a), green line] shows just a weak peak in the near infrared. Moreover, the reflectance is slightly increased over the entire range of wavelengths [see Fig. 3(b) for the visible wavelength range] but still shows a lower reflectivity for larger wavelengths compared to the scales' structure. We assume that this difference results from the struts oriented in the propagation direction of the light, which are present in the beetle scales but absent in our model and with a length of about 1 μm have a different size compared to the layer thickness.

High reflectance does not lead to whiteness automatically; hence, the quality of our model is evaluated by its color impression. Therefore, we investigate the coloring of the far-field for the refined model and the scales' structure provided by Wilts *et al.*[1] Since our model and the white beetle model [Figs. 3(c) and 3(d), respectively] exhibit qualitatively the same coloration, we conclude that our model shows the same whiteness as the beetle. The same calculation for the previous model with a fixed center-to-center distance also reveals a comparable coloration (not shown).

To assess the scattering strength, we calculate the TIS for both structures and yield TIS = 98.1% ± 0.4% and TIS = 96.0% ± 0.4% for the refined model and the beetle's structure, respectively (TIS = 97.6% ± 0.4% for the previous model). Thus, our model exhibits even a slightly higher scattering strength than its biological role-model. Compared to the *Morpho*-like structure shown in Fig. 1(b), the scattering is distinctly enhanced because of the increased disorder.

Another aspect investigated is the time-of-flight of a short light pulse transmitted through the scales since this measurement provides crucial information about light transport in disordered structures. Burresi *et al.* have found that the lifetime of light within the scales is roughly $\tau = 140$ fs for a beetle of the genus *Cyphochilus*.[3] We perform FDTD calculations to estimate the time-of-flight of a light pulse of the same length as used in the experiment through our refined model structure for comparison. According to the procedure provided by Burresi *et al.*, we fit the exponential decay of the transmitted light pulse and yield a lifetime of roughly τ = 140 fs in remarkable accordance with the experimental results [compare Fig. 3(e)]. Since the development of the *Morpho*-like model and the white beetle model starts with a similar base, our analysis verifies the assumption of Vukusic *et al.*: the narrow border between ordered structures producing strong coloration and highly scattering white structures can be crossed by increasing tailored disorder.[2]

III. CONCLUSION

Since our model can perfectly explain all so far investigated optical properties of the scales in the visible spectral range, we conclude that constructive interference and multiple light scattering between detuned Bragg stacks are the functional principle underlying the scales' structure. Moreover, the model demonstrates that the scales' structure can be derived from a strictly ordered structure by introducing disorder. This may open up the way to a better understanding of disordered structures in general as more of those may have an underlying ordered structure. Since the model with a fixed center-to-center distance already exhibits the same optical behavior for the visible wavelength range than the beetle scales' structure, the disorder of the scales' structure can be reduced without reducing the functionality in the visible wavelength range. Thus, this model improves the beetle scales in respect of producibility. Moreover, it shows a high reflectance for a certain but tunable infrared wavelength range, which is useful to reflect heat radiation and hence preventing overheating.

As the model is composed of a sequence of layers, 2.5D structuring techniques combined with stacking techniques might be used for fabrication. This allows fast and inexpensive large scale fabrication of white structures, which do not fade. This may open up a new way of white coloration.

IV. METHODS

A. Model parameters

All models are composed of stacks with a footprint of 300 nm × 300 nm. The lateral size of all models is 7 × 7 μm^2. The offsets for the pairs of adjacent stacks in the *Morpho*-like structure are chosen according to a Gaussian distribution with a mean value of μ = 30 nm and a standard derivation of σ = 20 nm in a range from 0 nm to 70 nm. The periodicity of the Bragg stack used as basis for the model mimicking the white beetle is $d = d_{\text{chitin}} + d_{\text{air}} = 587$ nm which corresponds to an optical path length of $d_{\text{opt}} = n_{\text{chitin}} d_{\text{chitin}} + d_{\text{air}} = 713$ nm. The spectral position of the stop band of a Bragg stack is given by $\lambda = 4 n_{\text{chitin}} d_{\text{chitin}}/(2j - 1)$ with $j \in \mathbb{N}$ leading to a fundamental stop band at $\lambda_{j=1}$ = 1426 nm and a second order stop band in the visible spectral range at $\lambda_{j=2}$ = 475 nm. Matlab (The Mathworld, Inc., USA) is used to calculate the Gaussian distribution of the thickness with a mean value of μ = 230 nm and a standard derivation of σ = 160 nm in a range from 50 nm to 600 nm and the distribution of the holes. In the refined model, the center-to-center distance is varied according to a Gaussian distribution with a mean value of μ = 587 nm and a standard deviation of σ = 100 nm in a range from 350 nm to 800 nm.

B. FDTD calculations

The propagation of electromagnetic waves through the different models is calculated using the FDTD technique[23,24] (software: FDTD Solutions, Lumerical, Inc., CA). The direction of the incident plane wave is perpendicular to the layers. The calculations are performed with periodic boundary conditions parallel to the propagation direction of light and with perfectly matched layer conditions in the propagation direction. The reflectance is calculated using a 2D monitor between the light source and the structure which records the fields of the incident and the backscattered waves. The monitor is perpendicularly oriented to the incident light.

C. Coloration of the far-field calculations

To calculate the coloration of the far-field, the spectral intensity distribution $I(\lambda)$ resulting from the FDTD simulation is used to compute the corresponding colors in the International Commission on Illumination (CIE) 1931 red-green-blue (RGB) color space.[25] With the color matching functions $\bar{r}(\lambda)$, $\bar{g}(\lambda)$, and $\bar{b}(\lambda)$ presented by Smith and Guild,[25] the RGB values without normalization can be computed according to

$$R = \int I(\lambda)\bar{r}(\lambda)\mathrm{d}\lambda\,, \tag{1}$$

$$G = \int I(\lambda)\bar{g}(\lambda)\mathrm{d}\lambda\,, \tag{2}$$

$$B = \int I(\lambda)\bar{b}(\lambda)\mathrm{d}\lambda\,. \tag{3}$$

Since the absolute brightness is not relevant to assess the coloration, the normalization can be chosen arbitrary. To compare the different white structures, the normalization is chosen in such a way that the average RGB value is the same for every calculation.

ACKNOWLEDGMENTS

We acknowledge support from the Deutsche Forschungsgemeinschaft DFG within the priority program 1839 "Tailored Disorder." We thank B. D. Wilts for providing us with the 3D reconstruction of the inner structure of a beetle wing scale.

[1] B. D. Wilts, X. Sheng, M. Holler, A. Diaz, M. Guizar-Sicairos, J. Raabe, R. Hoppe, S.-H. Liu, R. Langford, O. D. Onelli, D. Chen, S. Torquato, U. Steiner, C. G. Schroer, S. Vignolini, and A. Sepe, Adv. Mater. **30**, 1702057 (2018).
[2] P. Vukusic, B. Hallam, and J. Noyes, Science **315**, 348 (2007).
[3] M. Burresi, L. Cortese, L. Pattelli, M. Kolle, P. Vukusic, D. S. Wiersma, U. Steiner, and S. Vignolini, Sci. Rep. **4**, 6075 (2014).
[4] L. Cortese, L. Pattelli, F. Utel, S. Vignolini, M. Burresi, and D. S. Wierma, Adv. Opt. Mater. **3**, 1337 (2015).
[5] S. M. Luke, B. T. Hallam, and P. Vukusic, Appl. Opt. **49**, 4246 (2010).
[6] B. Wipfler, H. Pohl, M. I. Yavorskaya, and R. G. Beutel, Curr. Opin. Insect Sci. **18**, 60 (2016).
[7] D. J. Stokes, F. Morrissey, and B. H. Lich, J. Phys.: Conf. Ser. **26**, 50 (2006).
[8] B. T. Hallam, A. G. Hiorns, and P. Vukusic, Appl. Opt. **48**, 3243 (2009).
[9] J. Syurik, R. H. Siddique, A. Dollmann, G. Gomard, M. Schneider, M. Worgull, G. Wiegand, and H. Hölscher, Sci. Rep. **7**, 46637 (2017).
[10] J. Syurik, G. Jacucci, O. D. Onelli, H. Hölscher, and S. Vignolini, Adv. Funct. Mater. **28**, 1706901 (2018).
[11] P. Vukusic, J. R. Sambles, C. R. Lawrence, and R. J. Wootton, Proc. R. Soc. London, Ser. B **266**, 1403 (1999).
[12] S. Kinoshita, S. Yoshioka, and K. Kawagoe, Proc. R. Soc. B **269**, 1417 (2002).
[13] S. Kinoshita, S. Yoshioka, and J. Miyazaki, Rep. Prog. Phys. **71**, 076401 (2008).
[14] H. L. Leertouwer, B. D. Wilts, and D. G. Stavenga, Opt. Express **19**, 24061 (2011).
[15] K. Watanabe, T. Hoshino, K. Kanda, Y. Haruyama, and S. Matsui, Jpn. J. Appl. Phys., Part 2 **44**, L48 (2005).
[16] R. H. Siddique, S. Diewald, J. Leuthold, and H. Hölscher, Opt. Express **21**, 14351 (2013).
[17] J. E. Harvey, N. Choi, S. Schroeder, and A. Duparré, Opt. Eng. **51**, 013402 (2012).
[18] A. R. Parker, D. R. Mckenzie, and M. C. J. Large, J. Exp. Biol. **201**, 1307 (1998); http://jeb.biologists.org/content/201/9/1307#skip-link.
[19] A. R. Parker, J. Opt. A: Pure Appl. Opt. **2**, R15 (2000).
[20] A. L. Holt, A. M. Sweeney, S. Johnsen, and D. E. Morse, J. R. Soc., Interface **8**, 1386 (2011).
[21] T. M. Jordan, J. C. Partridge, and N. W. Roberts, J. R. Soc., Interface **11**, 20140948 (2014).
[22] J. A. Bossard, L. Lin, and D. H. Werner, J. R. Soc., Interface **13**, 20150975 (2016).
[23] K. S. Yee, IEEE Trans. Antennas Propag. **14**, 302 (1966).
[24] K. S. Yee and J. S. Chen, IEEE Trans. Antennas Propag. **45**, 354 (1997).
[25] T. Smith and J. Guild, Trans. Opt. Soc. **33**, 73 (1931).